MODELING AND REMOVING DEPTH VARIANT BLUR IN 3D FLUORESCENCE MICROSCOPY

Saima Ben Hadj and Laure Blanc-Féraud*

Morphème Research Group, I3S/CNRS/INRIA/UNSA/IBDC,
2000, route des Lucioles - Les Algorithmes - bât. Euclide B - BP 121,
06903 Sophia Antipolis Cedex, France.
e-mail: Saima.Ben_Hadj@inria.fr; Laure.Blanc_Feraud@inria.fr

ABSTRACT

Like many other imaging techniques, 3D fluorescence microscopy suffers from degradations that are basically varying with the depth of the point source. This is due to the light refraction phenomenon. In this article, we focus on modeling and removing depth variant blur in such a system. In particular, we study some of the existing space-variant blur approximations and consider an efficient approximation where the space variant blur function is a linear combination of a set of space-invariant ones. We then focus on restoring space-variant blurred images using such a model. For that, we fit a domain decomposition-based minimization approach to the deconvolution problem with a space variant blur model. We thus obtain a fast restoration algorithm where the image estimation is performed in a parallel way on different sub-images.

***Index Terms*—** Blur modeling, energy minimization, fluorescence microscopy, restoration, space-variant PSF, total variation.

1. INTRODUCTION

Even under the most suitable imaging conditions, optical images are affected by undesired blur mainly due to the inherent limitations of the optical instruments such as the light diffraction phenomenon. In order to enhance the optical image quality, a post computational processing such as deconvolution processing is needed. In this context, the blur is usually assumed to be space invariant (SI) and the image degradation modeling used is a convolution between the original image u and the system induced blur function h conventionally called Point Spread Function (PSF): $g(x) = \sum_{t\in\mathcal{O}} [h(x-t).u(t)] + b(x)$ where $b(.)$ is an additive noise and variables t and x are respectively locations in the object space $\mathcal{O}$ and the image space $\mathcal{I}$, sub-sets of $\mathbb{N}^3$. It is well known that the mathematical computations of such an operation can be rapidly carried out using fast Fourier transform. Nevertheless, in 3D fluorescence microscopy, the blur is essentially varying with depth due to the light refraction when crossing mediums of different refractive indexes. In this case, the image degradation process cannot anymore be modeled by a convolution. In fact, the mathematical observation model is now expressed as follows:

$$g(x) = \sum_{t\in\mathcal{O}} [h(x,t).u(t)] + b(x) \tag{1}$$

Because of the space-variance of the PSF, computations are very extensive in terms of CPU time and memory. In order to avoid fastidious computations, one solution consists in considering a piecewise invariant PSF in such a way that the convolution model is locally preserved. However, this leads to blur discontinuity artifacts in the resulting image and crudes approximations of the space-variant (SV) blur. To remedy this problem, we propose to use a convenient approximation of the continuously varying blur. In this article, we compare and assess the accuracy of two possible blur approximations presented in [1, 2, 3], in the particular case of 3D fluoscence microscopy. Afterwards, we invert this model by fitting a fast minimization method proposed in [4] to the restoration problem with a SV PSF. The energy minimization is processed in a parallel way on different areas of the image thanks to an overlapping domain decomposition strategy, leading to a fast algorithm. Our contribution consists in fitting this method to the case of SV PSF and showing that its convergence properties are preserved in the case of SV PSF. This article is organized as follows: the second section is devoted to study the approximate SV blur modeling. In the third section, we present the proposed restoration method. In the fourth section, we report and evaluate some numerical results obtained on a simulated 3D fluorescence microscopy image. Finally, we conclude this article by proposing some future work.

2. SPACE-VARIANT BLUR MODEL

In this section, we compare two main SV blur approximations i.e. the blur model proposed by Nagy et al in [1] and

(*) Thanks to ANR DIAMOND project for funding and interesting discussions between its partners.

the one proposed by Hirsch et al. in [3]. Both approximations are compared to the accurate theoretical model [5, 6] in the case of confocal laser scanning microscopy (CLSM) using some similarity criteria such as the structural similarity index (SSIM) [7] and the relative standard error (RSE). We then retain the most accurate one for the deblurring step.

2.1. Blur modeling proposed by Nagy et al., 1998

The blur model proposed in [1] is the following: $g(x) = \sum_{1 \le i \le D} \psi_i(x) \, . \, (h_i * u)(x)$ where ψ_i are nonnegative weighting functions such that $\sum_{1 \le i \le D} \psi_i(x) = 1$. The observation g is a SV linear combination of convolutions with SI PSF $h_i, \, 1 \le i \le D$. It is easy to show that the associated SV PSF is written as follows:

$$\widetilde{h}(x,t) = \sum_{1 \le i \le D} \psi_i(x) \, .h_i(x-t) \qquad (2)$$

Consequently, the proposed model is an interpolation in the image space of a given set of SI PSF.

2.2. Blur modeling proposed by Hirsch et al., 2010

A more recent SV blur model was proposed in [3] where: $g(x) = \sum_{1 \le i \le D} h_i * (\psi_i . u)(x)$ with $\psi_i(.)\,, \, 1 \le i \le D$, weighting functions as those considered in the previous subsection. We can show that the corresponding SV PSF is expressed as follows:

$$\widetilde{h}(x,t) = \sum_{1 \le i \le D} \psi_i(t) \, .h_i(x-t) \qquad (3)$$

Note that the model proposed in [2] for 3D fluorescence microscopy is a particular case of this modeling for particular weighting functions. Models (2) and (3) are used in (1) and differs in the argument of functions ψ_i.

2.3. Blur model assessment and selection

It is obvious that the two presented blur models are equivalent if we consider a piecewise-invariant PSF i.e. if the weighting function $\psi_i(x)$ is the indicator function for the i^{th} region (it equals 1 if x is in that region and 0 otherwise). However, in the general case, equations (2) and (3) leads to different blur functions. Although approximation (3) seems to be more natural as it allows to interpolate a given PSF set in the object space, it is difficult to say if one approximation is better than the other only based on these mathematical equations. That's why, we propose to solve this problem numerically by comparing these blur approximations for a given CLSM system. Let consider for instance a 3D image of size $200 \times 200 \times 190$ voxels composed of three micro-spheres. Axial slice (X, Z) of this image is displayed in Fig. 2 (a), Z being the depth variable along which the PSF is varying. We then generate a simulated image which is supposed to be distorted by a CLSM system (cf. Fig. 2 (b)). The 3D PSF is varying along the Z-direction (w.r.t depth) and is given by the theoretical PSF model of Stokseth [5]. We thus use this image as a reference. In order to generate approximate blur models as in (2) and (3), we should possess a set of PSF $\{h_i, \, 1 \le i \le D\}$ as well as convenient weighting functions $\{\psi_i, \, 1 \le i \le D\}$. For the PSF set generation, we use a method similar to that proposed in [8]. That is to say, PSF at different depths are computed using Stokseth model. Among these PSF functions, the set $\{h_i, \, 1 \le i \le D\}$ is selected such that no more than 15% of variation between two consecutive PSF (h_i and h_{i+1}) is tolerated. For the considered setting, we retain 10 PSF starting with the PSF at $0 \; \mu m$ to about $28.5 \; \mu m$ of depth. Weighting functions are chosen in order to interpolate two consecutive PSF. That is to say, we consider triangular functions displayed in Fig. 1 as those previously considered in [2, 8]. The peak of the weighting function ψ_i corresponds to the z-position of the selected PSF h_i. The blurred image according to models

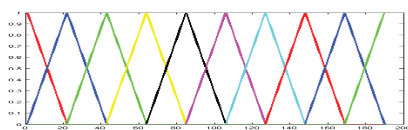

Fig. 1. Weighting function variation with depth.

(2) and (3) are respectively presented in Fig. 2 (c) and (d). To assess the proposed models, we depict in Fig. 2 (e) and (f) the absolute value of the error between each of the proposed approximate blurred images and the reference observation given by Fig. 2 (b). Moreover, we summarize in table 1 some other similarity measures such as the relative standard error (RSE) as well as the SSIM mean between each of the proposed models and the reference image. One can notice that for model (2), the RSE is very high, it is about 12.18% while it does not exceed 0.14% for model (3). This confirms the intuition that the model (3) is more accurate than that given by (2). Other comparative arguments are given in [9].

	Nagy et al.	Hirsch et al.
RSE (%)	12.18	0.14
SSIM mean	0.93	0.99

Table 1. Comparing SV blur models to the theoretical one.

3. IMAGE RESTORATION

Now, we are interested in inverting the second SV blur model proposed in [3] by minimizing an energy function formed by a quadratic term corresponding to data fidelity

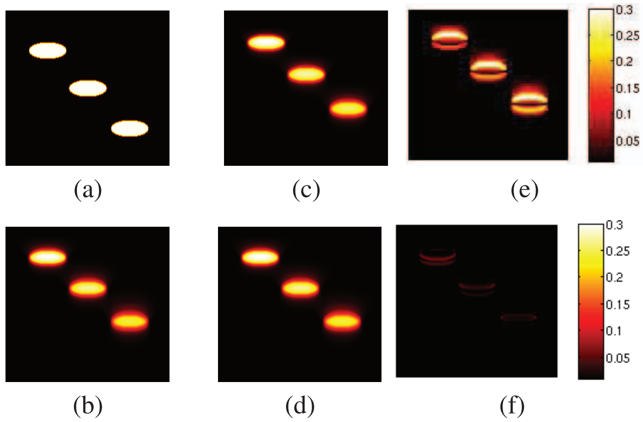

Fig. 2. (X, Z) slices of (a) the original 3D image, (b) the observation according to the theoretical model, (c) the blurred image using (2), (d) the blurred image using (3), (e) and (f) present the absolute value of the error between simulations respectively given by (2) and (3) and the reference image.

and a total variation regularization term that allows the smoothness of homogeneous areas while preserving edges: $J(u) = \left\|\widetilde{H}(u) - g\right\|_2^2 + 2\alpha \|\nabla u\|_1$ where $\alpha > 0$ is a fixed regularization parameter and $\widetilde{H}(u) = \sum_{1\leq i\leq D} H_i(\psi_i.u)$ with $H_i(.) = h_i * (.)$. In order to minimize such a function, we use an efficient and fast optimization method that was recently developed in [4] for linear filtering. In fact, the idea of this method consists in minimizing the function $J(.)$ in a parallel way on sub-domains of Ω in order to reduce the computational time. The image domain Ω is thus split into overlapping sub-domains, say for sake of clarity, a decomposition into two sub-domains Ω_1 and Ω_2 such that $\Omega = \Omega_1 \cup \Omega_2$ and $\Omega_1 \cap \Omega_2 \neq \varnothing$. Note that the number of sub-domains considered in the minimization method is not necessarily the same as that chosen for the PSF modeling. The solution u of the minimization problem is also split into partial solutions:
$$u(x) = \begin{cases} u_1(x) & if\, x \in \Omega_1 \setminus \Omega_2 \\ u_1(x) + u_2(x) & if\, x \in \Omega_1 \cap \Omega_2 \\ u_2(x) & if\, x \in \Omega_2 \setminus \Omega_1 \end{cases}$$
where the function u_i is in the subspace V_i, a set of functions whose support is in Ω_i. With this splitting, Fornasier et al. propose to perform the minimization of $J(.)$ in each sub-domain separately taking into account the estimate in the other sub-domain. The local minimization in each sub-domain is performed using *Lagrange multiplier* scheme. Details of the algorithm in the case of a SV PSF are given in [10]. This algorithm requires the knowledge of the adjoint of $\widetilde{H}$. We can easily prove that it is expressed as follows: $\widetilde{H}^*(.) = \sum_{1\leq i\leq D} \psi_i.H_i^*(.)$ with H_i^* the adjoint of H_i. Note that $\widetilde{H}^*(.)$ corresponds to the SV operator of model (2) and consequently, models (2) and (3) are adjoint to each other. Now, we check the convergence of the proposed minimization algorithm for the two non-stationary filters $\widetilde{H}$ and $\widetilde{H}^*$. The SI PSF used in each of these non-stationary filters are positive and normalized (i.e. $h_i(x) \geq 0, \forall x \in \Omega$ and $\sum_{x\in\Omega} h_i(x) = 1$). From the convergence proof established in [4], we exhibit two necessary conditions. First, the energy function $J(.)$ remains coercive for the considered SV operators. Indeed, when considering model (2), we can easily prove that this sufficient condition: function $f = 1 \notin Ker\left(\widetilde{H}^*\right)$, with $Ker\left(\widetilde{H}^*\right) = \left\{u \in \mathcal{H} : \widetilde{H}^*(u) = 0\right\}$ is satisfied [10]. It follows immediately from the fact that the SI PSF are normalized and the sum of weighting functions ψ_i is 1. For the second model (3), this property is also verified since $\widetilde{H}(1) = \sum_{1\leq i\leq D} H_i(\psi_i)$ is different from zero as ψ_i, $i = 1, ..., D$, are positive functions. A second necessary condition for the convergence of the proposed minimization method is $\left\|\widetilde{H}\right\|_2 < 1$ with $\| \widetilde{H} \|_2 = sup\left\{\| \widetilde{H}(u) \|_2 \; such\, that \; \| u \|_2 \leq 1\right\}$. Since $\left\|\widetilde{H}\right\|_2 = \left\|\widetilde{H}^*\right\|_2$, it suffices to prove that this property is verified for $\widetilde{H}^*$. It is obvious that the property $\|H\|_2 < 1$ is true for any normalized and stationary convolution operator H as long as it is normalized. Indeed, we can prove that $\|H\|_2 \leq \frac{1}{\sqrt{n}}$ with $n = Card(\Omega)$, using the properties of circulant matrix in the normalized Fourier transform domain (see [10] for details). Now, let prove this property ($\left\|\widetilde{H}^*\right\|_2 < 1$) for the SV operator $\widetilde{H}^*$. It is easy to show that any linear operator, even if it is SV, verifies: $\| \widetilde{H}^*(u) \|_2 \leq \sqrt{n} \; \| \widetilde{H}^*(u) \|_\infty$. Using the following triangle inequality: $\| \widetilde{H}^*(u) \|_\infty \leq \sup_{x\in\Omega} \sum_{i=1}^{D} |\psi_i(x)| . |H_i^*(u)(x)|$ and using the fact that $\forall x \in \Omega, 0 \leq \psi_i(x) \leq 1, \sum_{i=1}^{D} \psi_i(x) = 1$, and $|H_i^*(u)(x)| \leq \frac{1}{\sqrt{n}}$, we can show that $\| \widetilde{H}^*(u) \|_\infty \leq \frac{1}{\sqrt{n}}$. Thereby, we proved that $\left\|\widetilde{H}^*\right\|_2 = \left\|\widetilde{H}\right\|_2 \leq 1$. Up to a rescaling, the strict inequality can be obtained. By verifying these two conditions, the convergence proof follows analogous arguments as that presented in [4].

4. NUMERICAL RESULTS

We performed a first test of the proposed approach on the previously presented bead image of a CLSM system (see Fig. 2 (b)). To restore this image, we considered 10 PSF and weighting functions as those presented in Fig. 4 (a). (X, Z) slice of the restored image (cf. Fig. 3) as well as intensity profiles (cf. Fig. 4) along the optical axis passing through bead centers of the original object, the blurred one, the restored object with the proposed approach, and the restored object with the space-invariance assumption illustrate the relevance of the proposed method. In fact, the considered depth-variant blur model jointly takes into account the blur and the shift applied on the object. That's why, using the proposed approach, we succeed to remove the blur and retrieve the original bead positions (cf. Fig. 3 (d)). However, using a SI PSF computed at a zero depth in which the shift component is not taken into account, we only remove the blur. The algorithm converges after about 5 min for the considered image of size $200 \times 200 \times 190$ voxels and for a decomposition into two equi-sized sub-domains. Note that using the optimization method of Fornasier et al for a SI PSF, we gain about 30% of the computational time spent by a standard optimization method such as ADM [11]. Test are done on a machine having a multi-core processor (8 cores) of a frequency 1.86 GHz and the method was programmed in Matlab.

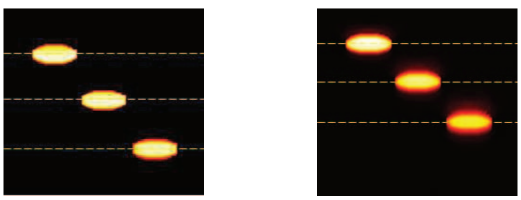

(a) (b)

Fig. 3. (X, Z) slices of the restored images (a) using a SV PSF and (b) using a SI PSF generated at a zero depth.

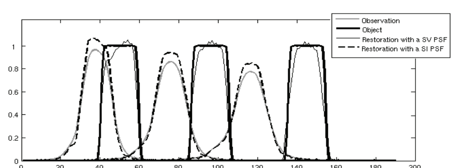

Fig. 4. Intensity profiles along Z-axis of the original object (black-bold), the observation (gray), the restorations using the SV PSF (black-fine) and using a SI PSF (discontinuous).

5. CONCLUSION

In this article, we presented a study of two main SV blur models [1, 3]. Based on some numerical results, we showed that the method proposed in [3] is a more accurate approximation of the SV blur in confocal microscopy. We then fitted the restoration method proposed in [4] to that model and showed its convergence properties. Test on simulated CLSM data showed promising results. We are currently applying this method on real data using experimental PSF. To conclude, further investigation concerns blind restoration in the context of the SV PSF model which is still an open issue.

6. ACKNOWLEDGMENT

The authors acknowledge Praveen Pankajakshan for clarifying many aspects about confocal microscopy and providing the theoretical PSF generation software. They also acknowledge Eric Thiébaut and his team for pointing out important and pertinent comparative properties of the SV blur models.

7. REFERENCES

[1] J.G. Nagy and D.P. O'Leary, "Restoring images degraded by spatially variant blur," *SIAM Journal on Scientific Computing*, vol. 19, no. 4, pp. 1063–1082, 1998.

[2] C. Preza and J.A. Conchello, "Depth-variant maximum-likelihood restoration for three-dimensional fluorescence microscopy," *JOSA A*, vol. 21, no. 9, pp. 1593–1601, 2004.

[3] M. Hirsch, S. Sra, B. Scholkopf, and S. Harmeling, "Efficient filter flow for space-variant multiframe blind deconvolution," in *IEEE CVPR*, 2010, pp. 607–614.

[4] M. Fornasier, A. Langer, and C.B. Schnlieb, "A convergent overlapping domain decomposition method for total variation minimization," *Numerische Mathematik*, pp. 1–41, 2009.

[5] P.A. Stokseth, "Properties of a defocused optical system," *JOSA*, vol. 59, no. 10, pp. 1314–1321, 1969.

[6] P. Pankajakshan, B. Zhang, L. Blanc-Féraud, Z. Kam, J.C. Olivo-Marin, and J. Zerubia, "Blind deconvoltion for thin layered confocal imaging," *Applied Optics*, vol. 48, no. 22, pp. 4437–4448, 2009.

[7] Z. Wang, A.C. Bovik, H.R. Sheikh, and E.P. Simoncelli, "Image quality assessment: From error visibility to structural similarity," *IEEE IP*, vol. 13, no. 4, pp. 600–612, 2004.

[8] E. Maalouf, "Contribution to fluorescence microscopy, 3d thick samples deconvolution and depth-variant psf," in *Ph.D. thesis, UHA*, Mulhouse, France, 2010.

[9] L. Denis, E. Thiébaut, and F. Soulez, "Fast model of space-variant blurring and its application to deconvolution in astronomy," in *IEEE ICIP*, Brussels, Belgium, Sept. 2011.

[10] S. Ben Hadj and L. Blanc-Féraud, "Restoration method for spatially variant blurred images," in *INRIA research report*, 2011, number 7654.

[11] M. Ng, P. Weiss, and Y. Xiaoming, "Solving constrained total-variation image restoration and reconstruction problems via alternating direction methods," *SIAM journal on scientific computing*, vol. 32, no. 5, pp. 2710–2736, 2011.